

Granular superconductors for high kinetic inductance and low loss quantum devices

Aviv Glezer Moshe,^{1, 2, a)} Eli Farber,² and Guy Deutscher¹

¹⁾*Raymond and Beverly Sackler School of Physics and Astronomy, Tel Aviv University, Tel Aviv 69978, Israel*

²⁾*Department of Physics and Department of Electrical and Electronic Engineering, Ariel University, P.O.B. 3, Ariel 40700, Israel.*

(Dated: August 10, 2020)

Granular aluminum is a promising material for high kinetic inductance devices such as qubit circuits. It has the advantage over atomically disordered materials such as NbN_x , to maintain a high kinetic inductance concomitantly with a high quality factor. We show that high quality nano-scale granular aluminum films having a sharp superconducting transition with normal state resistivity values of the order of $1 \times 10^5 \mu\Omega \text{ cm}$ and kinetic inductance values of the order of $10 \text{ nH}/\square$ can be obtained, surpassing state of the art values. We argue that this is a result of the different nature of the metal-to-insulator transition, being electronic correlations driven (Mott type) in the former and disorder driven (Anderson type) in the latter.

In recent years superconducting (SC) qubit circuits (QC) have evolved considerably. The first type, the so-called Cooper pair box^{1,2}, was basically composed of an island connected through a small Josephson junction (JJ) to a large pair reservoir, while a voltage V could be applied to it through a gate. States differing by one pair on the island could be weakly coupled through the JJ, creating a two-level system. More recently a different type of qubit, consisting of a small JJ shunted by a high inductance element, was developed to eliminate charge related noise and de-coherence. The large inductance element consisted originally of a one-dimensional array of large size JJ^{3,4}. More recently it was found that it could simply consist of a narrow line of a highly disordered superconductor such as NbN_x having a high kinetic inductance thanks to a low superfluid density⁵. Here it is virtual vortex tunneling through the narrow line that is the conjugate of the charge on the junction capacitance. It was however noted that formation of sub-gap states should be avoided in spite of disorder, as such states would introduce dissipation and thus de-coherence. We show here that nano-scale granular superconductors provide better solution because they are close to a Mott transition rather than to an Anderson transition, typical of atomic disorder, which induces a massive presence of sub-gap states.

When the mean free path l of a metal is reduced by disorder to be smaller than the BCS coherence length ξ_0 , the superfluid density n_s can be decreased substantially. For a given value of the current, pair velocity is much increased and the kinetic energy of the Cooper pairs becomes the dominant factor of the self-inductance of a stripe.

In a stripe of length L , width w and thickness t the kinetic energy of the superfluid with density n_s and velocity v_s is stored as inductive energy

$$n_s L w t \frac{1}{2} (2m) v_s^2 = \frac{1}{2} L_k I^2 \quad (1)$$

since $J_s = I_s / w t = n_s (2e) v_s$ and the penetration depth definition is $\lambda^2 = \frac{2m}{\mu_0 n_s (2e)^2}$ we obtain for the inductance

$$L_{k/\square} = \mu_0 \frac{\lambda^2}{t} \quad (2)$$

where $L_{k/\square}$ is the kinetic inductance divided by the number of squares L/w . Deep in the dirty limit, defined as $l \ll \xi_0$, $\lambda^2 \simeq \lambda_L^2 \xi_0 / l$, where λ_L is the London penetration depth⁶. Here λ_L is the penetration depth in the clean limit where $n_s = n/2$. Using the dirty limit expression for λ^2 and the BCS relation for $\xi_0 = \hbar v_F / \pi \Delta$ where v_F is the Fermi velocity and Δ is the SC gap, and taking into account that $l = v_F \tau$ where τ is the relaxation time, we obtain

$$L_{k/\square} = \frac{\hbar \rho_n}{\pi \Delta t} \quad (3)$$

where $\rho_n = m / n e^2 \tau$ is the normal state resistivity. In the BCS weak coupling $2\Delta = 3.53 k_B T_c$ ⁷ one can calculate $L_{k/\square}$ from the values of the sheet resistance $R_\square = \rho_n / t$ and the critical temperature.

A high inductance can be reached by increasing the value of the sheet resistance. This can be achieved by decreasing the film thickness (for example $\text{Nb}^{8,9}$), and/or by using a highly disordered metal such as NbN_x ^{5,10}, $\text{Nb}_x \text{Si}_{1-x}$ ¹¹, TiN^{12-15} and $\text{NbTiN}^{5,10-18}$. Because very thin films tend to be discontinuous the inductance values one can reach in this way are rather limited, of the order of a few pH per square⁹. Much higher values, of the order of 1 nH per square, have been reached by using strongly disordered films approaching the metal-to-insulator (M/I) transition, such as NbN_x ⁵. However it was found out that the quality factor of resonators made of such disordered films tends to deteriorate with disorder⁵. This has so far limited the use of disordered superconducting for high inductance devices, because higher losses mean increased de-coherence effects thus making quantum computing impractical.

Another material that has been considered recently for application in QC is granular aluminum (grAl)¹⁷⁻¹⁹. grAl films

^{a)}Electronic mail: avivmoshe@mail.tau.ac.il

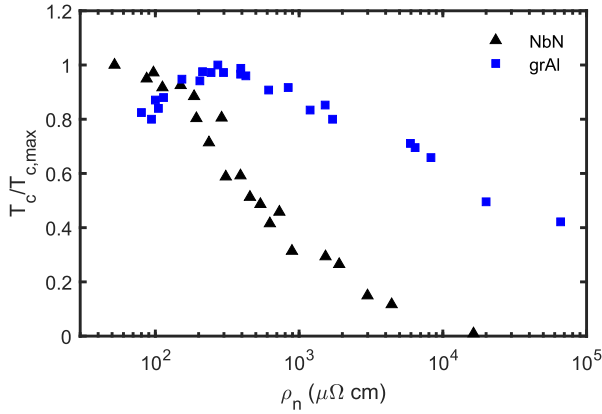


Figure 1. Variation of the critical temperature vs resistivity for 2 nm grain size samples. Black triangles are NbN_x data³¹ and blue squares are previously published grAl data²⁰ and our new data. The critical temperature values are normalized to their maximum of 16.69 K and 3.25 K, respectively. When superconductivity in NbN_x is quenched, it still persists up to relatively high resistivity values in nano-scale grAl. Note that even close to the metal-to-insulator transition the critical temperature of grAl is above that of pure bulk aluminum, which is marked by the value $T_c/T_{c,max} = 0.37$ in the figure.

can be prepared by thermally evaporating clean aluminum pellets in oxygen environment, for more details see²⁰. Their structure consists of small grains separated by aluminum oxide insulating barriers. The inter-grain coupling and resulting normal state resistivity are controlled by the oxygen partial pressure and Al deposition rate. High sheet resistance is reached by reducing inter-grain coupling rather than by atomic scale disorder. The phase diagram of T_c vs resistivity ρ_n has the well known “dome” shape, first rising to reach a maximum value which depends on the temperature of the substrate during film growth (respectively 2.3 K at room temperature^{21–24}, 3 nm grain size²², and 3.2 K at 100 K^{20,25–29}, 2 nm grain size with a narrower distribution^{29,30}) and thereafter decreasing as the metal-to-insulator transition is approached.

We show in Fig. 1 the decrease of T_c with resistivity of grAl films prepared as described above on liquid nitrogen cooled substrates. This decrease is slow. At a resistivity of $\sim 7 \times 10^4 \mu\Omega \text{ cm}$ T_c is still 40% of its maximum value. By contrast, the T_c of NbN_x films collapses much faster. They become useless for device applications at resistivity values of the order of less than $1 \times 10^4 \mu\Omega \text{ cm}$. grAl based devices can have kinetic inductance values one order of magnitude higher than NbN_x based devices, which represents a considerable advantage. Furthermore, we show in Fig. 2 that the superconductivity transition remains sharp up to the highest resistivity.

A further critical point concerns the level of losses, as seen for instance in resonators. In Fig. 3 we have collected values of internal quality factors reported for a number of devices as a function of their kinetic inductance values, with the aim of comparing devices based on atomically disordered super-

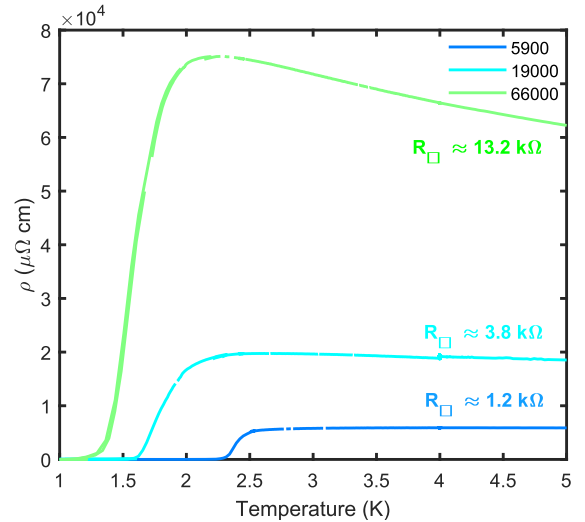


Figure 2. Resistance vs temperature curves of high resistivity films with 2 nm grain size. The legend corresponds to the normal state resistivity value in $\mu\Omega \text{ cm}$, taken as the value at 4.2 K. The corresponding value of the normal state sheet resistance is marked near each curve, exceeding the value $R_{\square} = h/(4e^2) \sim 6.5 \text{ k}\Omega$ for the highest resistance sample.

conductors such as NbN_x with grAl devices (here using films deposited at room temperature^{17,18,32}). The data shows a continuous decrease for the former, and no systematic change for the later. We emphasize that the highest kinetic inductance values reported in this figure are of about $1 \text{ nH}/\square$. This is because higher values cannot be reached for NbN_x and similar atomically disorder films, for the reasons explained above. However, in view of the high quality of our grAl films deposited at liquid nitrogen temperature as shown Fig. 2 we believe that values as high as $10 \text{ nH}/\square$ can be reached without increased losses.

We propose that the origin of the different behaviors of atomically disordered and granular superconductors lies in the different nature of their metal to insulator transition. When disorder is on the atomic scale the transition is of the Anderson type. This is the case in NbN_x films where disorder is created by introducing vacancies through a reduction of the nitrogen concentration^{31,33}. The density of states (DOS) of delocalized states decreases progressively to zero as more carriers near the Fermi level become localized. If the metal is a superconductor, the reduced DOS results in a fast decrease of the critical temperature. At the same time the localized carriers create sub-gap states such as two-level systems or collective modes such as the Higgs modes³⁴ and increased losses must be expected. An increased density of sub-gap states is intrinsic to the vicinity of an Anderson transition.

The nature of the metal-to-insulator transition is quite different in a granular metal consisting of nano-size metal crystallites weakly coupled together. When the coupling is weak enough, the Coulomb charging energy of the grains turns the granular system into an insulator^{35,36}. By analogy with the Hubbard case³⁷ the transition can be of the Mott type when

Material	$R_{\square}(\Omega)$	t (nm)	Q_i	L_k/\square (nH/ \square)
grAl ³²	20	20	1.7×10^5	0.016*
grAl ³²	40	20	$\sim 3 \times 10^4$	0.032*
grAl ³²	80	20	$\sim 1.5 \times 10^5$	0.064*
grAl ³²	110	20	$\sim 4 \times 10^5$	0.088*
grAl ³²	450	20	$\sim 10^5$	0.360*
grAl ³²	800	20	$\sim 2 \times 10^5$	0.640*
grAl ^{17,18}	2000	20	$\sim 10^5$	2
grAl ⁴¹	1645	26	$\sim 2 \times 10^4$	1.2
grAl ⁴¹	1661	25	$\sim 10^4$	1.2
grAl ⁴¹	2706	37	$\sim 10^4$	2
NbN _x ¹⁰	500	20	2.5×10^4	0.082*
NbN _x ⁵	2000	2-3	$\sim 10^3$	1.3
Nb _x Si _{1-x} (x=0.18) ¹¹	600	15	$10^3 - 10^4$	0.83
TiN ^{12,13}	25	40	$\sim 10^4 - 10^6$	0.008*
TiN ¹⁴	45	22	8.7×10^5	0.031*
TiN ¹⁵	600	6	$\sim 10^4$	0.620
TiN ⁴²	505	8.9	$(0.7 - 1) \times 10^5$	0.234*
TiN ⁴²	145	14.2	$(2 - 6) \times 10^5$	0.056*
TiN ⁴²	21	49.8	$(0.3 - 2) \times 10^6$	0.0071*
TiN ⁴²	6	109	$10^5 - 10^6$	0.0017*
NbTiN ¹⁶	250	8	$\sim 10^5$	0.035*

Table I. Internal quality factors Q_i at low circulating photon numbers, approaching single photon regime. Asterisk marks L_k/\square as estimated by Eq. 3 with the assumption of a BCS weak coupling ratio. Note that all grAl data shown in this table was taken for samples deposited onto substrates held at room temperature.

that energy is of the order of the effective band width of the granular system (determined by the strength of the inter-grain coupling), if disorder effects are not dominant. As discussed by Beloborodov *et al.*, disorder will in fact dominate if the spacing between the electronic levels in the individual grains is small³⁶. The spacing can be approximated by $\delta = 1/N(0)V$ ³⁸ where $N(0)$ is the DOS at the Fermi level and V is the grain volume. That spacing is indeed small in the Al-Ge system, in which the grain size is about 10 nm³⁹. The spacing being then of the order of 1 K. But when the grain size is about 2 nm, the inter-level spacing is about 100 K⁴⁰. If, in addition the grain size distribution is narrow as is the case here, a Mott transition can be preserved. Indeed, disorder appears to play in that case only a minor role since superconductivity persists up to $k_F l$ values smaller than unity²⁰. Additional experimental evidence for a Mott transition in nano-scale grAl has been previously presented and discussed²⁵.

In Fig. 4 we compare the optical conductivity versus frequency of the two systems for similar values of the resistivity. In high resistivity NbN_x samples the real part of the conductivity remains high below the gap value obtained from a fit

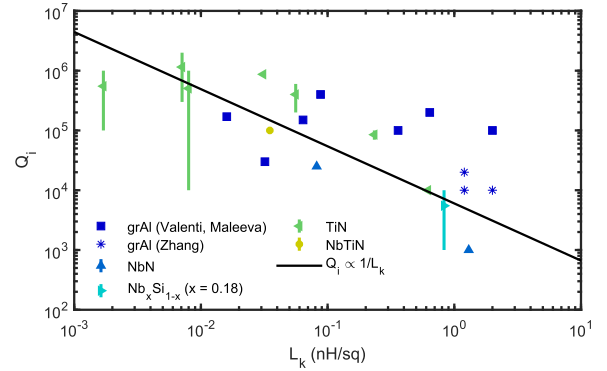


Figure 3. Internal quality factor Q_i vs. sheet kinetic inductance L_k/\square . For devices in which the Q_i values are widely distributed we represent the data as a thick vertical line. At high L_k/\square values devices based on grAl films have a higher Q_i than films of atomically disordered superconductors. Note that the data for grAl is from two different groups, represented by Zhang⁴¹ and Valenti, Maleeva^{18,32} in the legend.

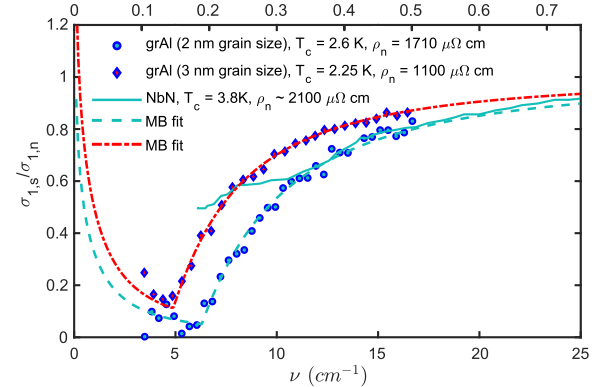


Figure 4. Comparison of the real part of the optical conductivity between grAl and NbN_x at temperature of 1.5 K. Circles are 2 nm grain size grAl data²⁰, diamonds are 3 nm grain size grAl data and full line is NbN_x data⁴³. For the grAl samples the fit to MB theory (dashed lines) works well all the way down to the gap value, marked by the minimum of σ_1 at 2Δ . For the NbN_x sample it does not. The frequency units are given in wavenumbers which are related to the angular frequency by $\omega = 2\pi c\nu$. Top axis frequency units are given in THz.

to Mattis-Bardeen (MB) theory⁴⁴ at high frequencies, indicating the massive presence of in-gap states. This deviation from MB is systematic for high resistivity low T_c NbN_x films^{34,43}. In strong contrast, in high resistivity grAl samples the fit to MB theory remains good down to low frequencies, for both grain sizes. The data for 3 nm grain size sample has been taken by us with the same setup as described in²⁰. The density of sub-gap states, if present, is evidently much lower than in NbN_x. The good agreement with the MB theory is in line with the measured temperature dependence of the change in resonance frequency $\delta f_0/f_0$ for a series of resonators made of grAl, with resistivities up to 1600 $\mu\Omega cm$, deposited onto substrates held at room temperature³².

The internal quality factor can be approximated by the expression $Q_i \simeq \sigma_2/\sigma_1$ which holds for thin film ($t \ll \lambda$) and a kinetic induction fraction $\alpha = L_k/L_g$ of order unity¹⁵. At frequencies below the gap, $\sigma_2 \propto 1/\omega$ and in the zero temperature limit the value of σ_1 is expected to approach zero for $\hbar\omega < 2\Delta$ (the data in Fig. 4 was taken at $T/T_c \sim 0.6-0.7$ for grAl and ~ 0.4 for NbN_x)⁴⁴. Therefore, the presence of sub-gap states for NbN_x suggests that a lower quality factor would be obtained than for grAl. A difference by two orders of magnitude in the quality factors as can be seen in Table I between grAl and NbN_x having a similar sheet resistance of 2000 Ω is therefore reasonable.

On the basis of these compared optical conductivity data we expect higher losses in devices based on NbN_x, and other atomically disordered superconductors, than in devices using nano-scale grAl. This is borne out by the respective quality factor values of resonators made of these two types of materials, see Table I. In atomically disordered superconductors the quality factor decreases as the sheet resistance and the related inductance increase, while resonators made of grAl have both a high inductance and a high quality factor.

Regarding the possibility of other Mott granular SC, we suggest granular materials having a level spacing of the order of 100 K. The advantage of grAl is that this criterion is established naturally during the sample evaporation, without any need for expensive techniques. Al-Ge films deposited at low temperature are also a possibility⁴⁵.

In summary, we suggest that the nature of the M/I transition is crucial for achieving both high kinetic inductance and high quality factor devices. Atomically disordered SC are less suitable for this purpose, as evident from the low quality factors which we believe result from massive presence of sub-gap states seen from optical conductivity data. In contrast, nano-scale superconductors, such as grAl, are more suitable for this purpose. Their higher quality factor at large kinetic inductance values results we believe from the absence of intrinsic sub-gap states. We have interpreted this difference as being due to the different nature of the metal-to-insulator transition in these two systems, being of the Anderson type in NbN_x and of the Mott type in nano-scale grAl. We suggest therefore that high inductance devices based on superconducting granular films, consisting of grains of only a few nano-meters with a narrow size distribution so as to reduce disorder effects, should be further considered for implementation in quantum circuits.

We acknowledge fruitful discussions with Ioan Pop, Florence Levy-Bertrand, Marc Scheffler, Nimrod Bachar and Christoph Strunk, held at the Superconducting Kinetic Inductances 2019 workshop in Bad Honnef, hosted by the Wilhelm and Else Heraeus-Foundation.

DATA AVAILABILITY

The data that supports the findings of this study are available within the article.

REFERENCES

- ¹V. Bouchiat, D. Vion, P. Joyez, D. Esteve, and M. H. Devoret, *Physica Scripta* **T76**, 165 (1998).
- ²Y. Nakamura, Y. A. Pashkin, and J. S. Tsai, *Nature* **398**, 786 (1999).
- ³J. E. Mooij, T. P. Orlando, L. Levitov, L. Tian, C. H. van der Wal, and S. Lloyd, *Science* **285**, 1036 (1999), <https://science.sciencemag.org/content/285/5430/1036.full.pdf>.
- ⁴V. E. Manucharyan, J. Koch, L. I. Glazman, and M. H. Devoret, *Science* **326**, 113 (2009), <https://science.sciencemag.org/content/326/5949/113.full.pdf>.
- ⁵J. T. Peltonen, O. V. Astafiev, Y. P. Korneeva, B. M. Voronov, A. A. Korneev, I. M. Charaev, A. V. Semenov, G. N. Golt'sman, L. B. Ioffe, T. M. Klapwijk, and J. S. Tsai, *Phys. Rev. B* **88**, 220506 (2013).
- ⁶M. Tinkham, *Introduction to Superconductivity: Second Edition*, Dover Books on Physics (Dover Publications, 2004).
- ⁷J. Bardeen, L. N. Cooper, and J. R. Schrieffer, *Physical Review* **108**, 1175 (1957).
- ⁸A. J. Annunziata, D. F. Santavicca, J. D. Chudow, L. Frunzio, M. J. Rooks, A. Frydman, and D. E. Prober, *IEEE Transactions on Applied Superconductivity* **19**, 327 (2009).
- ⁹A. J. Annunziata, D. F. Santavicca, L. Frunzio, G. Catelani, M. J. Rooks, A. Frydman, and D. E. Prober, *Nanotechnology* **21**, 445202 (2010).
- ¹⁰D. Niepce, J. Burnett, and J. Bylander, *Phys. Rev. Applied* **11**, 044014 (2019).
- ¹¹H. le Sueur, A. Svilans, N. Bourlet, A. Murani, L. Bergé, L. Dumoulin, and P. Joyez, arXiv e-prints, arXiv:1810.12801 (2018), arXiv:1810.12801 [cond-mat.supr-con].
- ¹²H. G. Leduc, B. Bumble, P. K. Day, B. H. Eom, J. Gao, S. Golwala, B. A. Mazin, S. McHugh, A. Merrill, D. C. Moore, O. Noroozian, A. D. Turner, and J. Zmuidzinas, *Applied Physics Letters* **97**, 102509 (2010), <https://doi.org/10.1063/1.3480420>.
- ¹³M. R. Vissers, J. Gao, D. S. Wisbey, D. A. Hite, C. C. Tsuei, A. D. Corcoles, M. Steffen, and D. P. Pappas, *Applied Physics Letters* **97**, 232509 (2010), <https://doi.org/10.1063/1.3517252>.
- ¹⁴L. J. Swenson, P. K. Day, B. H. Eom, H. G. Leduc, N. Llombart, C. M. McKenney, O. Noroozian, and J. Zmuidzinas, *Journal of Applied Physics* **113**, 104501 (2013), <https://doi.org/10.1063/1.4794808>.
- ¹⁵P. C. J. J. Coumou, M. R. Zuiddam, E. F. C. Driessen, P. J. de Visser, J. J. A. Baselmans, and T. M. Klapwijk, *IEEE Transactions on Applied Superconductivity* **23**, 7500404 (2013).
- ¹⁶N. Samkharadze, A. Bruno, P. Scarlino, G. Zheng, D. P. DiVincenzo, L. DiCarlo, and L. M. K. Vandersypen, *Phys. Rev. Applied* **5**, 044004 (2016).
- ¹⁷L. Grünhaupt, N. Maleeva, S. T. Skacel, M. Calvo, F. Levy-Bertrand, A. V. Ustinov, H. Rotzinger, A. Monfardini, G. Catelani, and I. M. Pop, *Phys. Rev. Lett.* **121**, 117001 (2018).
- ¹⁸N. Maleeva, L. Grünhaupt, T. Klein, F. Levy-Bertrand, O. Dupre, M. Calvo, F. Valenti, P. Winkel, F. Friedrich, W. Wernsdorfer, A. V. Ustinov, H. Rotzinger, A. Monfardini, M. V. Fistul, and I. M. Pop, *Nature Communications* **9**, 3889 (2018).
- ¹⁹P. Winkel, K. Borisov, L. Grünhaupt, D. Rieger, M. Spiecker, F. Valenti, A. V. Ustinov, W. Wernsdorfer, and I. M. Pop, arXiv e-prints, arXiv:1911.02333 (2019), arXiv:1911.02333 [quant-ph].
- ²⁰A. G. Moshe, E. Farber, and G. Deutscher, *Phys. Rev. B* **99**, 224503 (2019).
- ²¹F. Levy-Bertrand, T. Klein, T. Grenet, O. Dupré, A. Benoît, A. Bidaud, O. Bourrion, M. Calvo, A. Catalano, A. Gomez, J. Goupy, L. Grünhaupt, U. v. Luepke, N. Maleeva, F. Valenti, I. M. Pop, and A. Monfardini, *Phys. Rev. B* **99**, 094506 (2019).
- ²²G. Deutscher, H. Fenichel, M. Gershenson, E. Grunbaum, and Z. Ovadyahu, *Journal of Low Temperature Physics* **10**, 231 (1973).
- ²³R. W. Cohen and B. Abeles, *Phys. Rev.* **168**, 444 (1968).
- ²⁴R. C. Dynes, J. P. Garno, G. B. Hertel, and T. P. Orlando, *Phys. Rev. Lett.* **53**, 2437 (1984).
- ²⁵N. Bachar, S. Lerer, A. Levy, S. Hacohe-Gourgy, B. Almog, H. Saadaoui, Z. Salman, E. Morenzoni, and G. Deutscher, *Physical Review B* **91**, 041123 (2015).
- ²⁶N. Bachar, S. Lerer, S. Hacohe-Gourgy, B. Almog, and G. Deutscher, *Physical Review B* **87**, 214512 (2013).
- ²⁷U. S. Pracht, N. Bachar, L. Benfatto, G. Deutscher, E. Farber, M. Dressel, and M. Scheffler, *Physical Review B* **93**, 100503 (2016).

- ²⁸U. S. Pracht, T. Cea, N. Bachar, G. Deutscher, E. Farber, M. Dressel, M. Scheffler, C. Castellani, A. M. García-García, and L. Benfatto, *Physical Review B* **96**, 094514 (2017).
- ²⁹G. Deutscher, M. Gershenson, E. Grunbaum, and Y. Imry, *Journal of Vacuum Science and Technology* **10**, 697 (1973).
- ³⁰S. Lerer, N. Bachar, G. Deutscher, and Y. Dagan, *Physical Review B* **90**, 214521 (2014).
- ³¹M. Mondal, A. Kamlapure, M. Chand, G. Saraswat, S. Kumar, J. Jesudasan, L. Benfatto, V. Tripathi, and P. Raychaudhuri, *Phys. Rev. Lett.* **106**, 047001 (2011).
- ³²F. Valenti, F. Henriques, G. Catelani, N. Maleeva, L. Grünhaupt, U. von Lüpke, S. T. Skacel, P. Winkel, A. Bilmes, A. V. Ustinov, J. Goupy, M. Calvo, A. Benoît, F. Levy-Bertrand, A. Monfardini, and I. M. Pop, *Phys. Rev. Applied* **11**, 054087 (2019).
- ³³M. Chand, G. Saraswat, A. Kamlapure, M. Mondal, S. Kumar, J. Jesudasan, V. Bagwe, L. Benfatto, V. Tripathi, and P. Raychaudhuri, *Phys. Rev. B* **85**, 014508 (2012).
- ³⁴D. Sherman, U. S. Pracht, B. Gorshunov, S. Poran, J. Jesudasan, M. Chand, P. Raychaudhuri, M. Swanson, N. Trivedi, A. Auerbach, M. Scheffler, A. Frydman, and M. Dressel, *Nature Physics* **11**, 188 (2015).
- ³⁵B. Abeles, *Physical Review B* **15**, 2828 (1977).
- ³⁶I. S. Beloborodov, A. V. Lopatin, V. M. Vinokur, and K. B. Efetov, *Rev. Mod. Phys.* **79**, 469 (2007).
- ³⁷A. Georges, G. Kotliar, W. Krauth, and M. J. Rozenberg, *Rev. Mod. Phys.* **68**, 13 (1996).
- ³⁸R. Kubo, *Journal of the Physical Society of Japan* **17**, 975 (1962).
- ³⁹A. Gerber, A. Milner, G. Deutscher, M. Karpovsky, and A. Gladkikh, *Phys. Rev. Lett.* **78**, 4277 (1997).
- ⁴⁰N. Bachar, A. Levy, T. Prokscha, A. Suter, E. Morenzoni, Z. Salman, and G. Deutscher, *Phys. Rev. B* **101**, 024424 (2020).
- ⁴¹W. Zhang, K. Kalashnikov, W.-S. Lu, P. Kamenov, T. DiNapoli, and M. Gershenson, *Phys. Rev. Applied* **11**, 011003 (2019).
- ⁴²A. Shearrow, G. Koolstra, S. J. Whiteley, N. Earnest, P. S. Barry, F. J. Heremans, D. D. Awschalom, E. Shirokoff, and D. I. Schuster, *Applied Physics Letters* **113**, 212601 (2018), <https://doi.org/10.1063/1.5053461>.
- ⁴³B. Cheng, L. Wu, N. J. Laurita, H. Singh, M. Chand, P. Raychaudhuri, and N. P. Armitage, *Phys. Rev. B* **93**, 180511 (2016).
- ⁴⁴D. C. Mattis and J. Bardeen, *Phys. Rev.* **111**, 412 (1958).
- ⁴⁵A. Fontaine and F. Meunier, *Physik der kondensierten Materie* **14**, 119 (1972).